GREEN'S THEOREM DEGHOSTING ALGORITHMS IN (k,ω) (E.G., P-Vz DEGHOSTING) AS A SPECIAL CASE OF (x,ω) ALGORITHMS (BASED ON GREEN'S THEOREM) WITH: (1) SIGNIFICANT PRACTICAL ADVANTAGES AND DISADVANTAGES OF ALGORITHMS IN EACH DOMAIN, AND (2) A NEW MESSAGE, IMPLICATION AND OPPORTUNITY FOR MARINE TOWED STREAMER, OCEAN BOTTOM AND ON-SHORE ACQUISITION AND APPLICATIONS

ARTHUR B. WEGLEIN[1], JAMES D. MAYHAN[1], LASSE AMUNDSEN[2], HONG LIANG[1], JING WU[1], LIN TANG[1], YI LUO[3] and QIANG FU[1]

[1] *M-OSRP, University of Houston, 617 Science & Research Bldg. 1, Houston, TX, 77004-5005, U.S.A. aweglein@central.uh.edu*
[2] *Statoil Research Centre, Norway, and The Norwegian University of Science and Technology, Dept. of Petroleum Engineering and Applied Geophysics, Trondheim, Norway. lam@statoil.com*
[3] *Saudi Arabian Oil Company, EXPEC Advanced Research Center, Dhahran, Saudi Arabia. yi.luo@aramco.com*

(Received May 30, 2013; revised version accepted August 6, 2013)

ABSTRACT

Weglein, A.B., Mayhan, J.D., Amundsen, L., Liang, H., Wu, J., Tang, L., Luo, Y. and Fu, Q., 2013. Green's theorem deghosting algorithms in (**k**,ω) (e.g., P-V_z deghosting) as a special case of (**x**,ω) algorithms (based on Green's theorem) with: (1) significant practical advantages and disadvantages of algorithms in each domain, and (2) a new message, implication and opportunity for marine towed streamer, ocean bottom and on-shore acquisition and applications. *Journal of Seismic Exploration*, 22: 389-412.

This paper is examining the implications and differences of Green's theorem derived methods for deghosting in (**x**,ω) and (**k**,ω). Substituting for P_n a relationship with V_z in the (**k**,ω) method, and benefits and limitations that arise from that substitution (while important) are not within the scope of this paper. We point out how industry standard P-V_z deghosting (in **k**,ω) can be derived from Green's theorem deghosting (in **x**,ω). We discuss the advantages and disadvantages of deghosting methods for each domain. For example, the Green's theorem deghosting in (**x**,ω) can accommodate an arbitrary measurement surface, whereas P-V_z deghosting requires the source and field locations to be on a horizontal measurement surface. We discuss the implications of each deghosting/wavefield separation method for towed-streamer, ocean-bottom and on-shore acquisition.

KEY WORDS: deghosting, offshore processing, on-shore processing, Green's theorem, pre-processing.

0963-0651/13/$5.00

INTRODUCTION

We start with the meaning of deghosting, and the simplest up-down separation idea. Then, we show how those early simple ideas and thinking have evolved and advanced through methods based on Green's theorem. We then show explicitly how these recent advances reduce to the original, and readily accessible and understandable concepts and algorithms, and the advantages and disadvantages, and delivery that the original and more recent progress represent.

We will connect Green's theorem $(\mathbf{x},\omega)$ deghosting to the industry standard P-V_z method. P and P_n are the pressure and the normal derivative of pressure, respectively, and V_z is the vertical component of particle velocity. The industry standard P-V_z deghosting method will be shown to correspond to a Green's theorem method in $(\mathbf{k},\omega)$ where P_n is expressed in terms of V_z. In this paper, we will often refer to the Green's theorem deghosting method in $(\mathbf{k},\omega)$ as the P-V_z method. We will show a more direct way to derive that connection relationship than appears in Appendix B of Mayhan and Weglein (2013). We start with what resides behind the industry standard type of deghosting algorithm, review the Green's theorem deghosting method in $(\mathbf{x},\omega)$, and then show how the industry standard $(\mathbf{k},\omega)$/P-V_z method is a special case of the more general Green's theorem $(\mathbf{x},\omega)$ deghosting method. The $(\mathbf{x},\omega)$ method can derive the $(\mathbf{k},\omega)$ method as a special case, but not the other way around, i.e., the $(\mathbf{k},\omega)$ method cannot derive the $(\mathbf{x},\omega)$ method. approach. We point out how the P-V_z form method has advantages over Green's theorem in $(\mathbf{k},\omega)$ for on-shore application where the source is on the receiver measurement surface and the interest is in deghosting the data you acquired on the cable. The Green's theorem $(\mathbf{x},\omega)$ deghosting method has advantages over P-V_z when the receiver/source acquisition is not on a horizontal surface.

Events that go up (from the source) and/or down (from the free surface) can destructively interfere with non-ghosted events putting notches in the data, which are not in the source spectrum. Deghosting removes destructive interference and boosts low frequencies. Removing the downwave recorded by the receiver, we want to be left with an upwave, which is up/down separation. In addition to the traditional interests in deghosting described above, we prefer to deghost data prior to calling upon the inverse series to remove free surface multiples. Primaries, free surface multiples, and internal multiples are defined as events in the deghosted part of the measured wave field.

ELEMENTARY/ESSENTIAL LESSONS FOR DEGHOSTING THAT RELATE DATA ACQUISITION CHOICES AND STABLE SOLUTIONS

Consider a simple 1D normal incidence example, where in the vicinity of the (towed streamer) cable the pressure field P satisfies:

$$[(\partial^2/\partial z^2) - (1/c_0^2)(\partial^2/\partial t^2)]P = 0 \quad , \tag{1}$$

where c_0 is the wave speed in water, and

$$[(d^2/dz^2) + (\omega^2/c_0^2)]P = 0 \quad , \tag{2}$$

is the temporal Fourier transform of eq. (1). The solution of eq. (2) is

$$P = \underbrace{A\exp(ikz)}_{\text{down}} + \underbrace{B\exp(-ikz)}_{\text{up}} \quad , \tag{3}$$

where the convention $\exp(-i\omega t)$ is used for going from ω to t. For deghosting, we want to up-down separate P at the assumed measurement location $z = a$. That requires two pieces of information about P.

Two measurements at one depth

If we make the required two pieces of information about P measurements of the field and its derivative at one level, for a cable at $z = a$,

$$P(a) = A\exp(ika) + B\exp(-ika)$$

$$P'(a) = ik[A\exp(ika) - B\exp(-ika)] \quad ,$$

Solve for B,

$$B = \{[ikP(a) - P'(a)]/2ik\}\exp(ika) \quad ,$$

and the upgoing wave at $z = a$ is

$$[ikP(a) - P'(a)]/2ik \quad .$$

If we extend the above to a multi-D world in the vicinity of the cable,

$$[\nabla^2 - (1/c_0^2)\partial_t^2]P(x,z,x_s,z_s,t) = 0 \quad . \tag{4}$$

In the temporal Fourier domain, eq. (4) becomes

$$(\nabla^2 + k^2)P(x,z,x_s,z_s,\omega) = 0 \quad ,$$

and then Fourier transforming over x we have

$$[(d^2/dz^2) + k^2 - k_x^2]P(k_x,z,x_s,z_s,\omega) = 0 \quad . \tag{5}$$

Taking $q^2 \equiv k^2 - k_x^2$, eq. (5) looks like eq. (2). The solution of eq. (5) is

$$P = A\exp(iqz) + B\exp(-iqz) \ ,$$

where A, B are functions of k_x and ω, whereas in eq. (3), A, B are functions of ω. We get B the same way as before except that the role of k will be played by q, i.e., in the prestack form [eq. (5)] the deghosted data at the cable (at z = a) is

$$P_r(a,k_x,\omega) = [iqP(a,k_x,\omega) - P'(a,k_x,\omega)]/2iq \ , \qquad (6)$$

with $q = +\sqrt{\{(\omega/c_0)^2 - k_x^2\}}$.

When P′ is substituted with $i\omega\rho V_z$ where ρ is the local mass density at the cable and V_z is the vertical component of velocity, eq. (6) becomes

$$P_r(a,k_x,\omega) = [iqP(a,k_x,\omega) - i\omega\rho V_z(a,k_x,\omega)]/2iq \ , \qquad (7)$$

the receiver deghosted data on the cable at z = a. The latter formula is the prototype of industry standard P-V_z summation for deghosting.

Two measurements at two depths

Another way to provide two pieces of information about P is to use P on the cable and P at the free surface (where P = 0). We get

$$P(0) = A + B \ , \qquad (8a)$$

$$P(a) = A\exp(ika) + B\exp(-ika) \ . \qquad (8b)$$

To solve for B, multiply eq. (8a) by exp(ika) and subtract eq. (8b) to get

$$\exp(ika)P(0) - P(a) = B[\exp(ika) - \exp(-ika)] \ ,$$

$$B = [\exp(ika)P(0) - P(a)]/[\exp(ika) - \exp(-ika)]$$

$$= [\exp(ika)P(0) - P(a)]/[2i\sin(ka)] \ , \qquad (9)$$

which in principle is entirely equivalent to eq. (7), but can have stability issues compared to eq. (7) for small errors in the cable depth, especially in the vicinity of notches. This was noted in Mayhan and Weglein (2013). To illustrate, let's assume that the total wave is upgoing and it doesn't require deghosting. Then the measured wave is P(z) = P(0)exp(−ikz). Then put P(a) into eq. (9) to get

$$B = [\exp(ika)P(0) - \overbrace{P(0)\exp(-ika)}^{P(a)}]/[\exp(ika) - \exp(-ika)] = P(0) \quad ,$$

the deghosted data at $z = 0$; if the depth is correct, then the exponentials [exp(ika) − exp(−ika)] in the numerator and denominator cancel for any frequency and there's no problems. But, if you have the cable depth wrong (the cable is at 'a' but you think it's at 'b'), the exponentials don't cancel, and you can get zeros in the denominator.

There is no sensitivity in eq. (7) to division. Eq. (7) is the solution for B with two measurements at one depth, while eq. (9) is the same formula for B with two measurements at two depths. In theory eqs. (7) and (9) are equivalent, but in practice eq. (9) can have issues. Zhang (2007) shows that for a small error in depth eq. (7) is stable. For typical towed streamer data at 6 m, a receiver notch occurs at 125 Hz. This frequency is usually outside your data (e.g., with max 70 Hz). But if you're collecting data to 250 Hz, the notch is in your data. The zeros are at $ka = n\pi$, or $k = n\pi/a$, $n = 0,1,2,\ldots$ If you make the cable deeper, the notches shift to lower frequencies. At the ocean bottom, the notches can come in at 5 Hz. Deghosting is very serious for ocean bottom data, because the notches are inside your data. Eq. (7) is two measurements (field and its derivative) at one level. That's what Green's theorem depends on, $(P\nabla' G_0 - G_0\nabla' P)\cdot\hat{n}$ on the measurement surface.

GREEN'S THEOREM

There are many applications of Green's theorem in seismic processing; among them are wavefield separation and wavefield prediction methods. Green's theorem deghosting is a wavefield separation concept and method. The Green's theorem based marine deghosting method begins with a description of (the waves in) the actual medium in terms of a whole space reference medium of water plus three sources located on different sides of the measurement surface. See Fig. 1 and Zhang (2007) and Mayhan and Weglein (2012). One source converts water to air, ρ_{air}, one source corresponds to the air guns, $\rho_{airguns}$, and one source converts water to earth, ρ_{earth}. With this homogeneous reference medium, the causal whole-space Green's function, G_0^{d+}, from a source to the field point is always outgoing and straight away from the source.

The differential equation for the total pressure field, P, in this reference medium/sources description is

$$(\nabla^2 + k^2)P = \rho_{air} + \rho_{airguns} + \rho_{earth} \quad .$$

Consider the integral, I, defined as

$$I(\mathbf{r},\omega) = \oint [P(\mathbf{r}',\mathbf{r}_s,\omega)\nabla' G_0^{d+}(\mathbf{r},\mathbf{r}',\omega) - G_0^{d+}(\mathbf{r},\mathbf{r}',\omega)\nabla' P(\mathbf{r}',\mathbf{r}_s,\omega)]\cdot\hat{n}dS' \quad . \tag{10}$$

where S is a closed surface whose lower surface is the measurement surface and the upper surface is a large radius hemisphere above the measurement surface. When eq. (10) is evaluated at a point **r** inside the volume V it gives the contribution due to the sources outside V on the field at a point inside V. When the integral, eq. (10), is evaluated at a point r above the cable and below the air guns, $\omega_{airguns}$, the wave due to the 'earth' is upgoing, whereas the waves from the 'air guns' and the 'air' are downgoing. Hence, at that point the integral in eq. (10) provides the upgoing portion of the total measured wavefield, and hence is the receiver deghosted portion of the total wavefield at **r**. We therefore call $I(\mathbf{r},\omega)$ the receiver deghosted data, $P_r(\mathbf{r},\omega)$. With the description of three sources and the whole space reference medium, the integral in eq. (10) gives the portion of the total wavefield due to the source ρ_{earth}. At that point, **r**, the portions of the total wave due to the other two sources are downgoing.

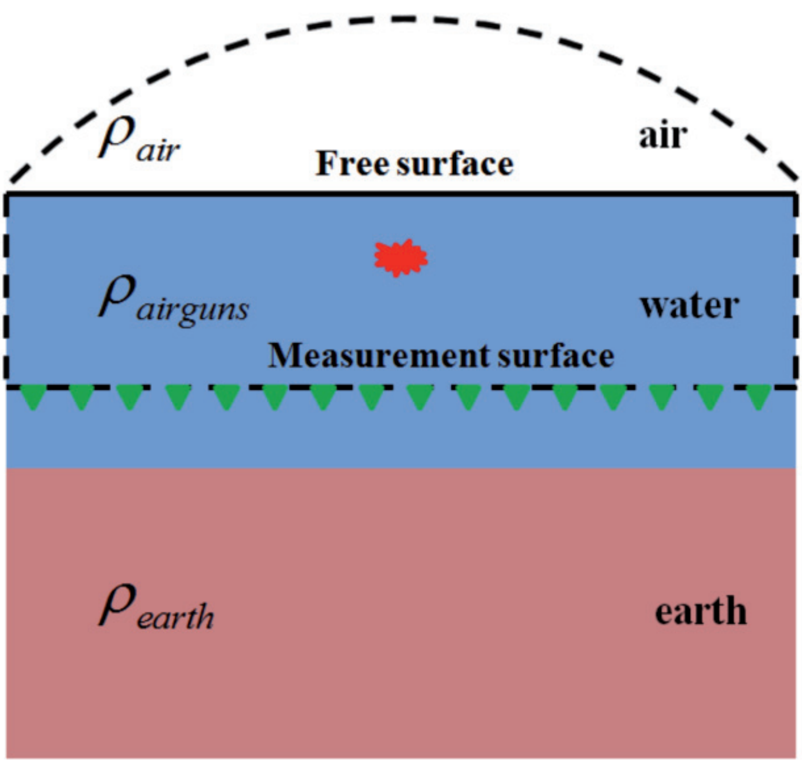

Fig. 1. Configuration for Green's theorem deghosting. ρ_{air}, $\rho_{airguns}$, and ρ_{earth}, overlay the reference medium (whole space of water) to give the actual medium. The closed surface of integration is the dashed line.

DERIVING P-V_z FROM GREEN'S THEOREM

We now start with eq. (10) and derive eq. (7), the latter being the basis of P-V_z deghosting. We provide the derivation in 2D, and the 3D derivation is a straightforward generalization. Let (x',z') be the receiver coordinates, i.e., x' runs along the cable and z' is the constant depth of the cable, (x_s,z_s) is the source location, and (x,z) is the prediction point, where we choose for deghosting $z_s < z < z'$. The integral [in eq. (10)] produces an upwave at (x,z), which outputs the receiver deghosted field at the point (x,z).

Eq. (9) depends on measurements at two depths, i.e., the cable depth and the free surface. The integral [in eq. (10)] relates to eq. (7). Advances in acquisition have allowed eq. (10) to be realized in practice. Writing eq. (10) in 2D,

$$P_r(x,z,x_s,z_s,\omega) = \int dx'[P(x',z',x_s,z_s,\omega)(\partial/\partial z')G_0^{d+}(x,z,x',z',\omega) - G_0^{d+}(x,z,x',z',\omega)(\partial/\partial z')P(x',z',x_s,z_s,\omega)] \quad , \qquad (11)$$

where the left hand side is the receiver deghosted portion of P. The next steps in this derivation benefit from the work of Corrigan et al. (1991), Amundsen (1993) and Weglein and Amundsen (2003). Fourier transforming eq. (11) with respect to x gives

$$\int \exp(-ik_x x)dx\, P_r(x,z,x_s,z_s,\omega) = \int \exp(-ik_x x)dx \int dx' \times [P(x',z',x_s,z_s,\omega)(\partial/\partial z')G_0^{d+}(x,z,x',z',\omega) - G_0^{d+}(x,z,x',z',\omega)(\partial/\partial z')P(x',z',x_s,z_s,\omega)] \quad , \qquad (12)$$

where G_0^{d+} is the causal whole space solution of

$$(\nabla^2 + k^2)G_0^{d+}(\mathbf{r},\mathbf{r}',\omega) = \delta(\mathbf{r} - \mathbf{r}') \quad . \qquad (13)$$

Substitute the bilinear form of the Green's function

$$G_0^{d+}(\mathbf{r},\mathbf{r}',\omega) = \int [1/(2\pi)^3][\exp(-i\mathbf{k}'\cdot\mathbf{r}')/(-|\mathbf{k}'|^2+k^2+i\varepsilon)]\exp(i\mathbf{k}'\cdot\mathbf{r})d\mathbf{k}' \quad . \qquad (14)$$

This bilinear form is the plane wave decomposition of G_0. Eq. (14) requires all wavenumbers to produce a single temporal frequency wave solution in a region that includes the source. Why does a single temporal frequency solution, G_0, require all $\mathbf{k}'$? The driving function, the Dirac delta function [in eq. (13)], contains all wavenumbers. So the solution with that driving function,

G_0, depends on all wavenumbers, as well. In 2D,

$$G_0(x,z,x',z',\omega) = [1/(2\pi)^2] \int \{\exp(ik_x'[x - x'])\exp(ik_z'[z - z'] \\ / (-k'^2 + k^2 + i\varepsilon)\}dk_x'dk_z' \ .$$

Fourier transform G_0 with $\int \exp(-ik_x x)dx$,

$$\underbrace{\int dx \exp(-ik_x x)\exp(ik_x' x)}_{2\pi\delta(k_x - k_x')}\exp(-ik_x' x')\exp(ik_z' x')\exp(ik_z'[z - z']) \ ,$$

and the Dirac delta allows you to carry out $\int dk_x'$

$$\exp(-ik_x x') \int \{\exp(ik_z'[z - z'])/(-k_x^2 - k_z'^2 + k^2 + i\varepsilon)\}dk_z' \ . \quad (15)$$

The integral looks like a 1D Green's function if we define $k^2 - k_x^2 \equiv q^2$. The latter relation between q, k_x and k is not due to a dispersion relationship but by introducing and defining the quantity q.

The 1D causal solution to

$$[(d^2/dz^2) + k^2]G_0 = \delta \ ,$$

is

$$G_0^+ = [\exp(ik|z - z'|)]/2ik \ . \quad (16)$$

The integral in eq. (15) then results in:

$$[\exp(iq|z - z'|)]/2iq \ ,$$

from eq. (16), and eq. (15) becomes

$$\exp(-ik_x x')[\exp(iq|z - z'|)]/2iq \ .$$

Now differentiate eq. (15) with respect to z',

$$[iq\,\mathrm{sgn}(z' - z)/2iq]\exp(iq|z - z'|)\exp(-ik_x x') \ .$$

The other term [in eq. (11)] will have G_0 with no derivative. Performing the integral over x' we then find

$$P_r(k_x,z,x_s,z_s,\omega) = P(k_x,z',x_s,z_s,\omega)[\mathrm{sgn}(z' - z)/2]\exp(iq|z - z'|) \\ - P'(k_x,z',x_s,z_s,\omega)[\exp(iq|z - z'|)]/2iq \ . \quad (17)$$

It's a combination of P and P′ at z′ (the measurement depth). Note there is no sum and no integral. The output point is shallower than the cable, $z' > z$, so $\mathrm{sgn}(z' - z) = 1$ and $|z - z'| = z' - z$, and we get the form eq. (7). This is called P-V_z deghosting.

The industry standard practice replaces P′, the normal derivative of P, with displacement in terms of the vertical component of velocity using the idea sketched here. Start with a 1D Newton's second law:

$$F = ma \quad ,$$

and in the frequency domain

$$F = mi\omega V_z \quad ,$$

where $a = i\omega V_z$ and V_z is the vertical component of velocity. This becomes

$$F/A = (m/A)i\omega V_z \quad ,$$

where A is "area".

$$P' \sim (1/l)(F/A) \sim (\partial/\partial z)(F/A) = (m/Al)i\omega V_z = \rho i\omega V_z \quad , \tag{18}$$

where $\rho = m/(Al)$ is the mass density. The Fourier transform turns the integral into a single product (diagonalizes an integral eq. (10) into an algebra expression with single products of terms). Eq. (17) with eq. (18) for P′ is the industry standard and called P-V_z summation. Why are we interested in a Green's theorem solution [eq. (10)] in $(\mathbf{x},\omega)$ when eqs. (17) and (18) are available?

1. The $(\mathbf{k},\omega)$ methods, eqs. (17) and (18), assume that you have adequate sampling and aperture to perform an effective/accurate Fourier transform. In practice in the crossline direction, it can be a challenge to perform a Fourier transform because crossline receivers are further apart than inline receivers and crossline aperture is limited compared to inline. Green's theorem in $(\mathbf{x},\omega)$ allows you to directly input and integrate the data you have recorded. Careful attention to implementation [e.g., Nyquist frequencies, padding to implement in $(\mathbf{k},\omega)$] is required for both methods.

2. Only Green's theorem deghosting in $(\mathbf{x},\omega)$ can perform a curved line (2D) or non-flat surface integral (3D) on the ocean bottom or onshore and can directly accommodate a non-horizontal cable. Ghosts are particularly important at the ocean bottom because the notches arrive at lower frequencies and typically within the seismic bandwidth.

We have shown that Green's theorem deghosting in $(\mathbf{x},\omega)$ relates to the industry standard $(\mathbf{k},\omega)$ method when the measurement surface is horizontal and the data in the space domain is adequate to perform Fourier transforms. Green's theorem in $(\mathbf{x},\omega)$ and in $(\mathbf{k},\omega)$ or P-V_z are not the same for a curved boundary. Green's theorem deghosting in $(\mathbf{x},\omega)$ is directly applicable to any shape or form of measurement surface whereas deghosting in $(\mathbf{k},\omega)$ or P-V_z is not. However, if the stringent requirements of $(\mathbf{k},\omega)$ are (assumed to be) satisfied then the $(\mathbf{k},\omega)$ deghosting method offers (within its assumptions) opportunities for on-shore and ocean bottom deghosting not available with $(\mathbf{x},\omega)$ methods. Details to explain and exemplify this statement are presented in the following section.

In the following two sections, several numerical comparisons will be given to see the results from the two methods (Green's theorem in $(\mathbf{x},\omega)$ and in $(\mathbf{k},\omega)$ or P-V_z) with different spatial sampling intervals and apertures. In order to study their isolated effects, for each test we keep one factor unchanged and only vary the other factor. A simple horizontal model (Fig. 2) is used for the tests. Since the second reflector is very deep, only the reflections from the first reflector are in the synthetic record. The acquisition geometry is listed in each figure. To avoid aliasing, low-pass filtering was applied in each experiment before de-ghosting. Regarding the trace number on the vertical axis in Figs. 3 to 14, the original synthetic data used for the tests has 1601 traces with a sampling interval of 3 m; trace 801 is the zero-offset trace. And trace 1000 means the trace with offset of 3 m $\times$ 200 = 600 m. Other trace numbers can be changed to offsets in a similar fashion. The time axes differ in the figures so as to make events in the figures clearer for purposes of comparison. The red lines in Figs. 3 through 14 are exact up-going waves without receiver side ghosts, and they can be used to examine the results of both methods. If the blue or green lines match well with the red ones, the results are satisfactory. From Figs. 3 to 8, by increasing the spatial sampling intervals from 3 m to 100 m, it can be seen that the blue and green lines better match the red one for smaller intervals. Similarly, from Figs. 9 to 14, the results are improved for wider apertures.

Numerical examples: Spatial sampling interval

First, we test/compare the results from the two different methods from changing the spatial sampling interval. To some extent, dense sampling reflects the situation of acquisition in the in-line direction, while sparse sampling is to mimic acquisition in the cross-line direction. Here we keep the aperture of 2400 m and increase the spatial sampling interval gradually, from 3 m to 30 m to 100 m. The single traces extracted from the gathers are shown in Figs. 3 through 8. In each figure, the red line represents the upgoing wave generated by using the Cagniard-de Hoop method, which can produce analytically accurate receiver side deghosted data. It can be used as a standard to verify the accuracy of the two deghosting methods. In each figure, the blue line represents the receiver-side deghosted result by using the $(\mathbf{k},\omega)$ domain method, while the green line is for the result by using the $(\mathbf{x},\omega)$ domain method. If the blue line or the green line matches well with the red line, the result is satisfactory. Besides single traces, the average spectrums are also used for further comparisons. The single traces extracted from the gathers and their average spectra are shown in Figs. 3 to 8.

Numerical examples: Aperture

Second, we test/compare the results from the two different methods when changing the aperture. Here, we keep the spatial sampling interval of 3 m and decrease the aperture gradually from 2400 m to 150 m to 45 m. The lines in Figs. 9 to 14 have the same meanings as the first part (above).

Numerical examples: Conclusions

Given a horizontal measurement surface, with careful attention to implementation, there is no practical difference between the (x,y,ω) and (k_x,k_y,ω) methods in terms of sampling and aperture requirements. Both methods represent wave theory processing (and neither is an asymptotic method), and, hence, both equally benefit from and appreciate wider apertures and denser sampling.

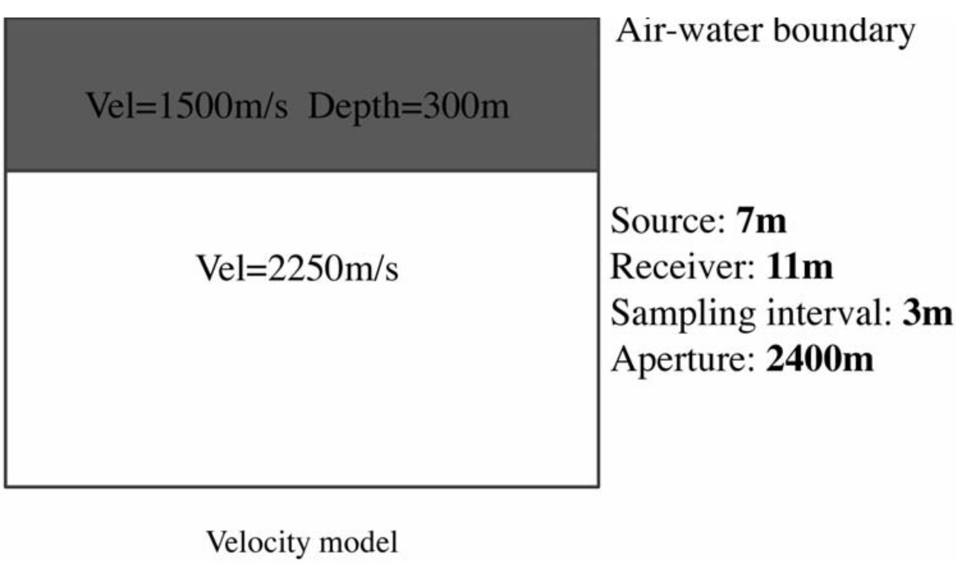

Fig. 2.

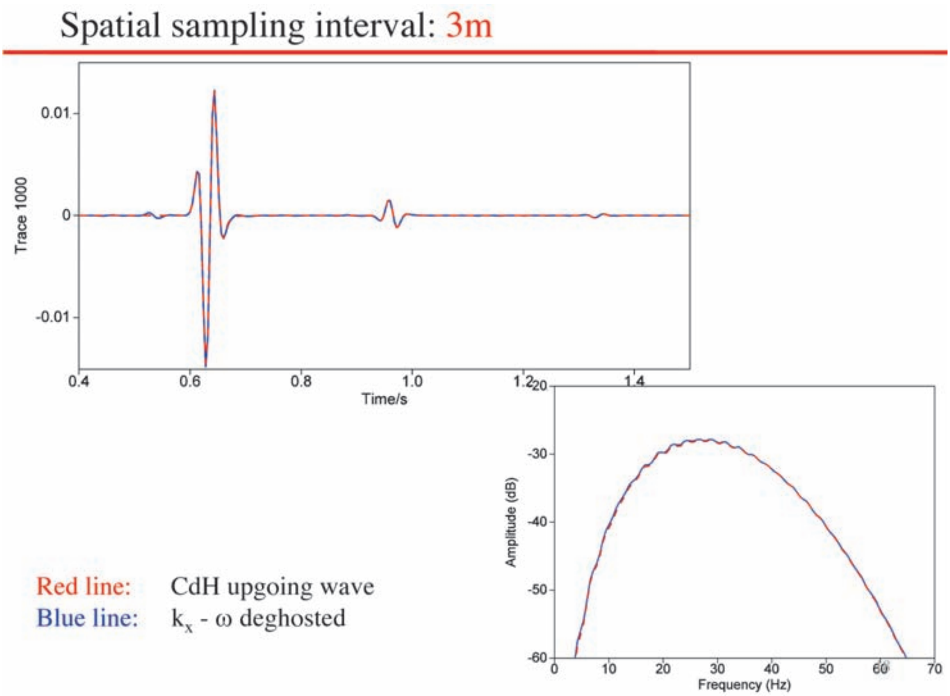

Spatial sampling interval: 3m
0.01
0
-0.01
Trace 1000
0.4
0.6
0.8
1.0
1.2
1.4
Time/s
-20
-30
-40
-50
-60
Amplitude (dB)
0
10
20
30
40
50
60
70
Frequency (Hz)
Red line: CdH upgoing wave
Blue line: k_x - ω deghosted

Fig. 3.

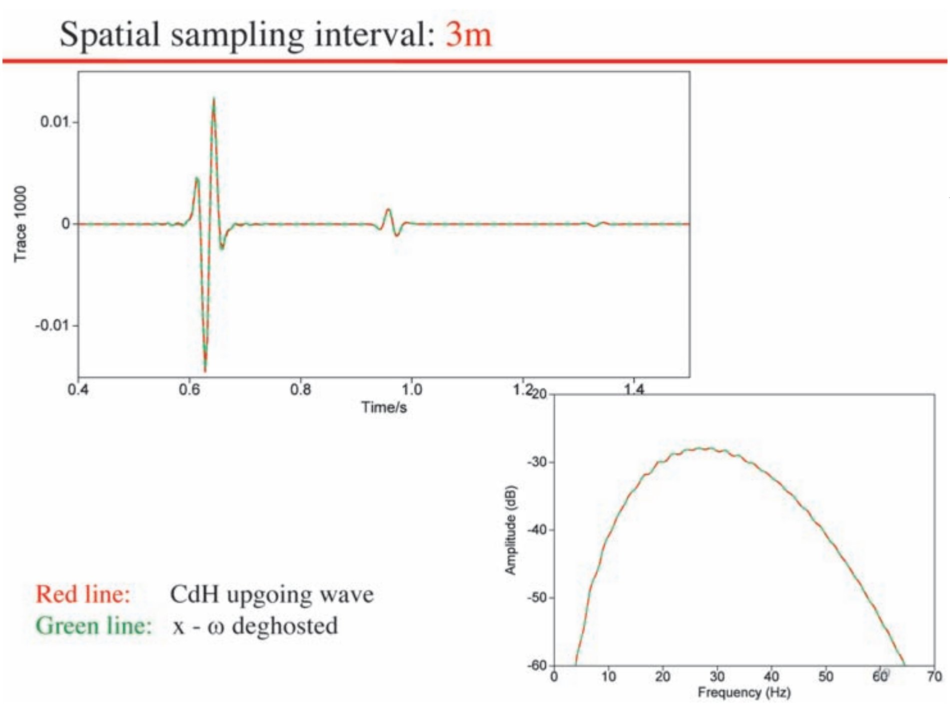

Spatial sampling interval: 3m
0.01
0
-0.01
Trace 1000
0.4
0.6
0.8
1.0
1.2
1.4
Time/s
-20
-30
-40
-50
-60
Amplitude (dB)
0
10
20
30
40
50
60
70
Frequency (Hz)
Red line: CdH upgoing wave
Green line: x - ω deghosted

Fig. 4.

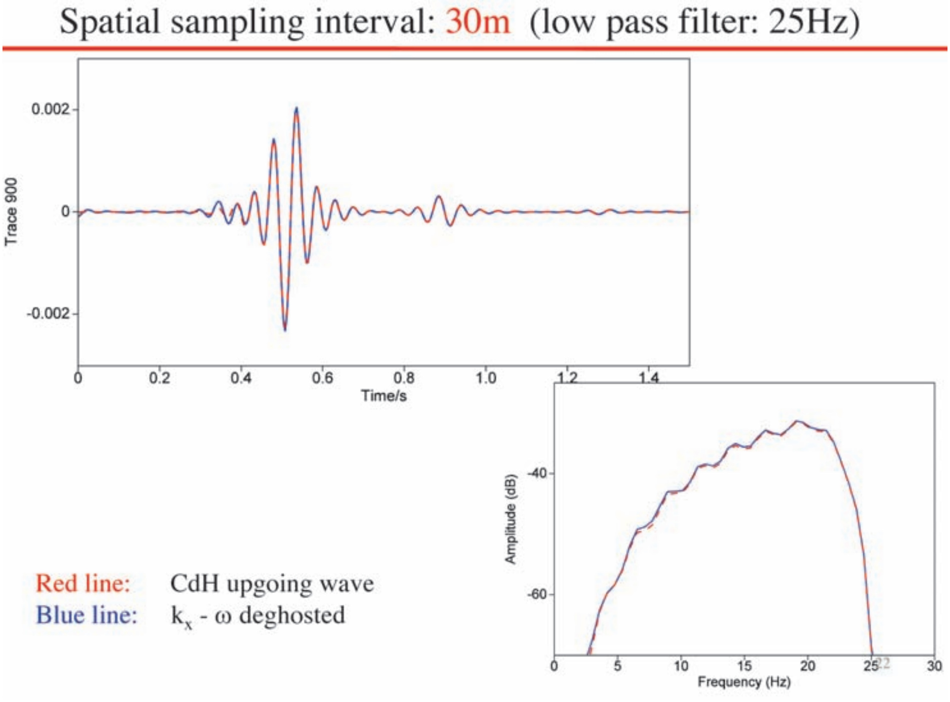
Spatial sampling interval: 30m (low pass filter: 25Hz)
Trace 900
Time/s
Amplitude (dB)
Frequency (Hz)
Red line: CdH upgoing wave
Blue line: k_x - ω deghosted

Fig. 5.

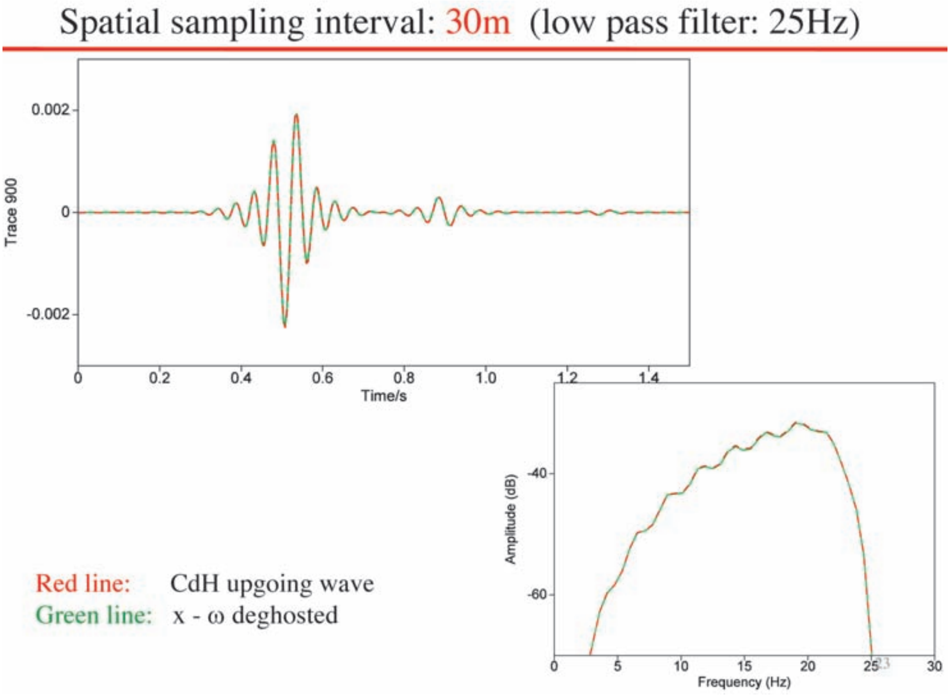
Spatial sampling interval: 30m (low pass filter: 25Hz)
Trace 900
Time/s
Amplitude (dB)
Frequency (Hz)
Red line: CdH upgoing wave
Green line: x - ω deghosted

Fig. 6.

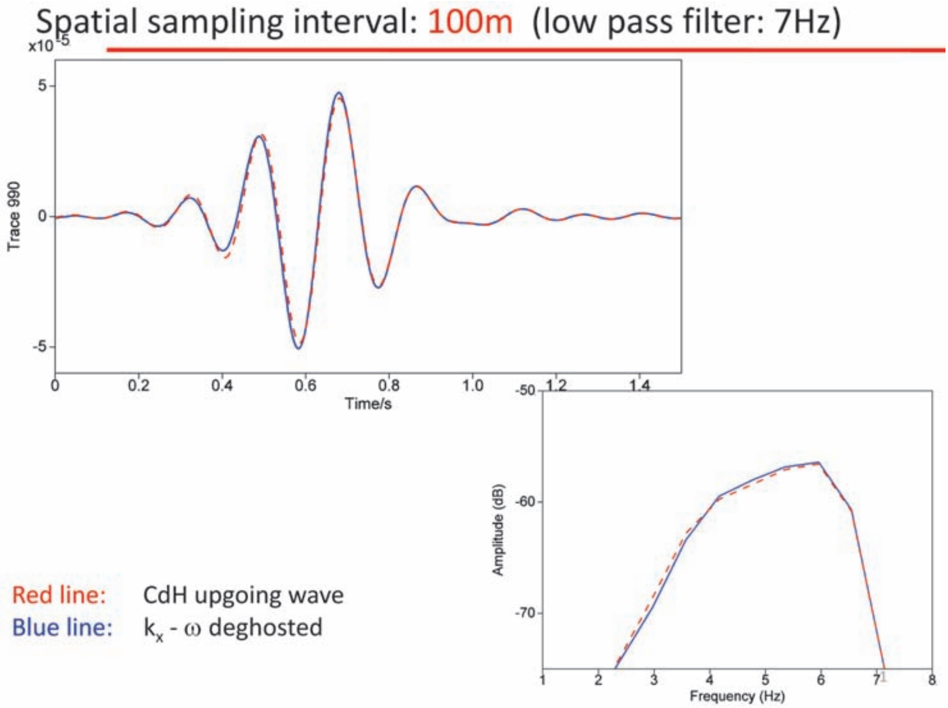
Spatial sampling interval: 100m (low pass filter: 7Hz)
x10^-5
Trace 990
Time/s
Amplitude (dB)
Frequency (Hz)
Red line: CdH upgoing wave
Blue line: k_x - ω deghosted

Fig. 7.

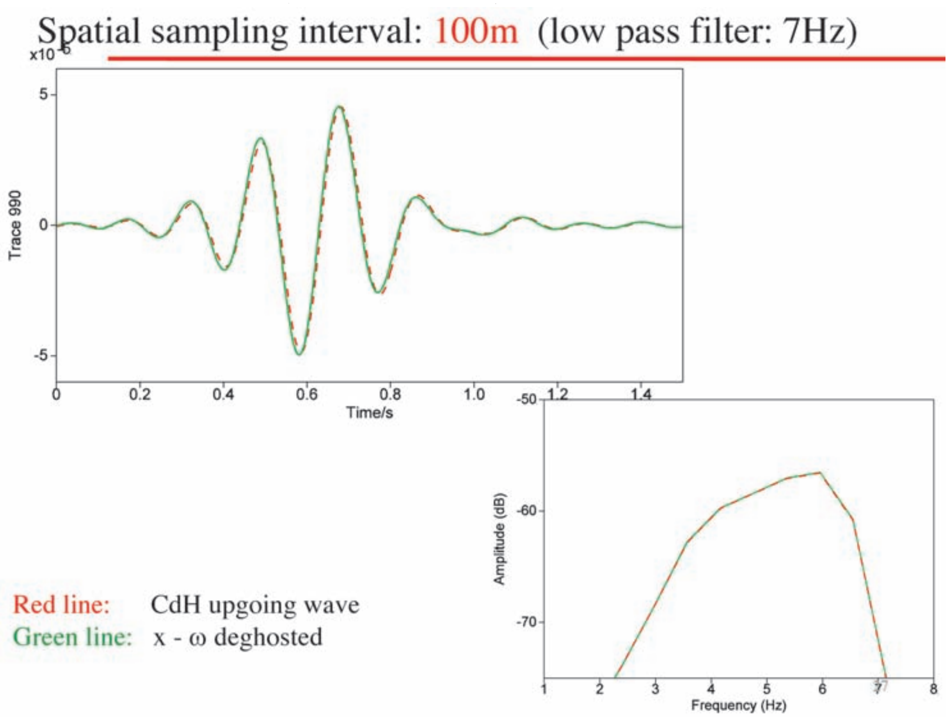
Spatial sampling interval: 100m (low pass filter: 7Hz)
x10^-5
Trace 990
Time/s
Amplitude (dB)
Frequency (Hz)
Red line: CdH upgoing wave
Green line: x - ω deghosted

Fig. 8.

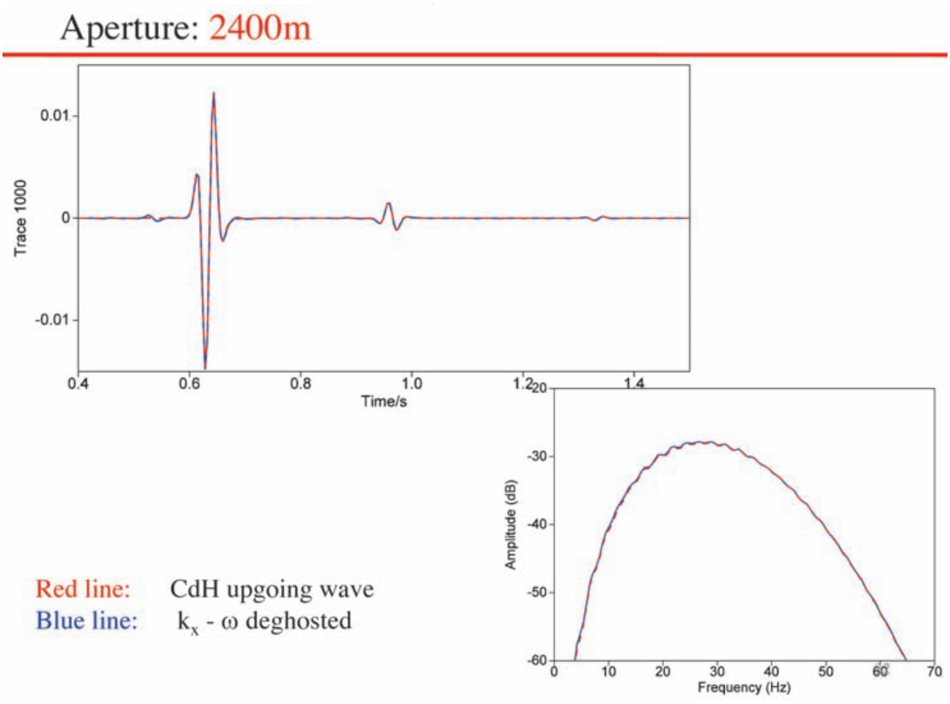
Aperture: 2400m
0.01
0
-0.01
Trace 1000
0.4
0.6
0.8
1.0
1.2
1.4
Time/s
Red line: CdH upgoing wave
Blue line: k_x - ω deghosted
-20
-30
-40
-50
-60
Amplitude (dB)
0
10
20
30
40
50
60
70
Frequency (Hz)

Fig. 9.

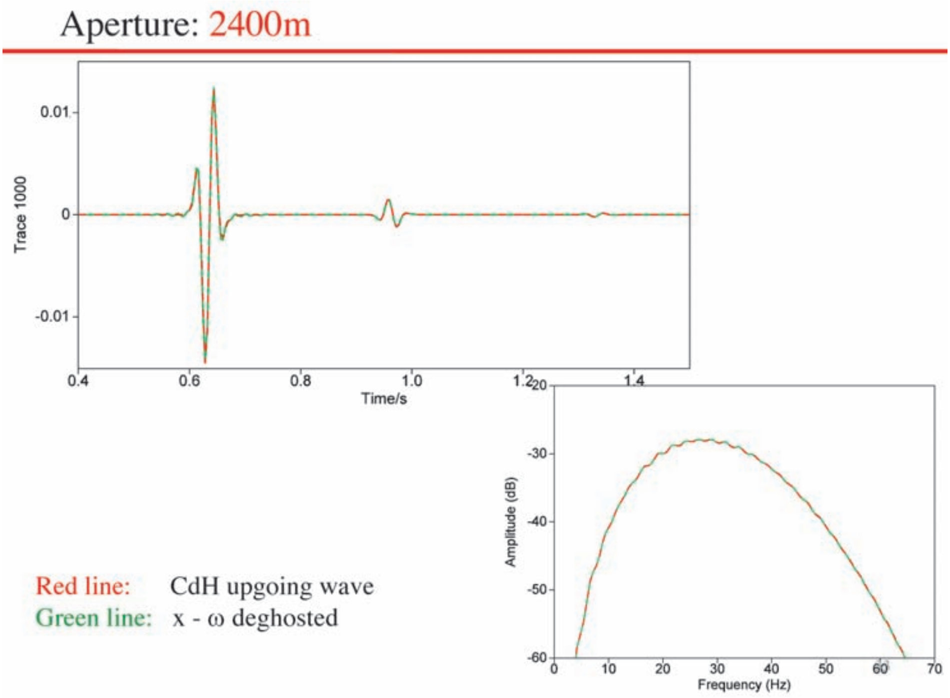
Aperture: 2400m
0.01
0
-0.01
Trace 1000
0.4
0.6
0.8
1.0
1.2
1.4
Time/s
Red line: CdH upgoing wave
Green line: x - ω deghosted
-20
-30
-40
-50
-60
Amplitude (dB)
0
10
20
30
40
50
60
70
Frequency (Hz)

Fig. 10.

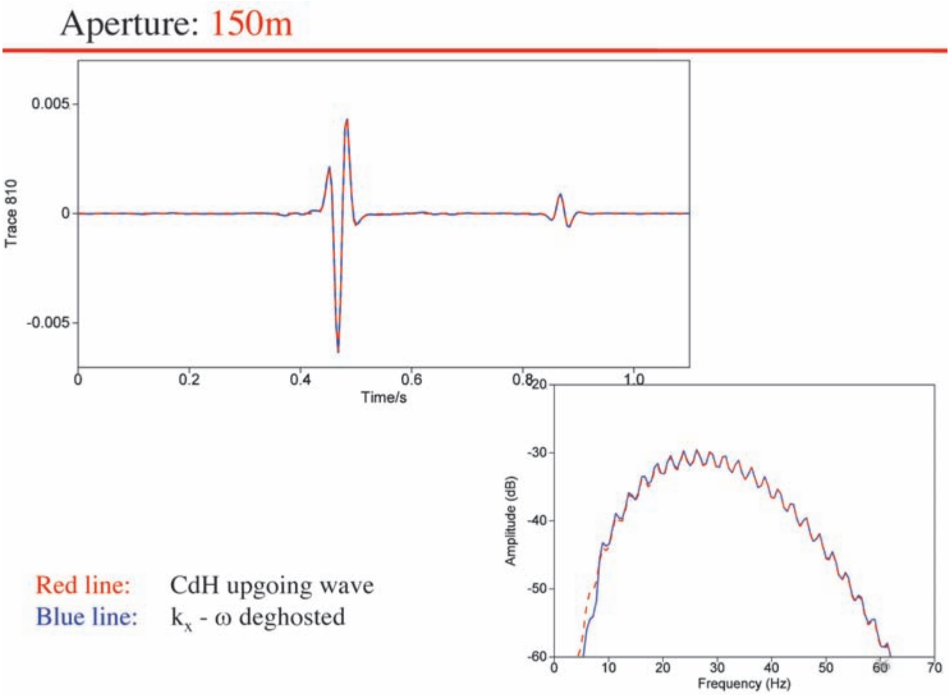
Aperture: 150m
0.005
0
-0.005
Trace 810
0
0.2
0.4
0.6
0.8
1.0
Time/s
Red line: CdH upgoing wave
Blue line: k_x - ω deghosted
-20
-30
-40
-50
-60
Amplitude (dB)
0
10
20
30
40
50
60
70
Frequency (Hz)

Fig. 11.

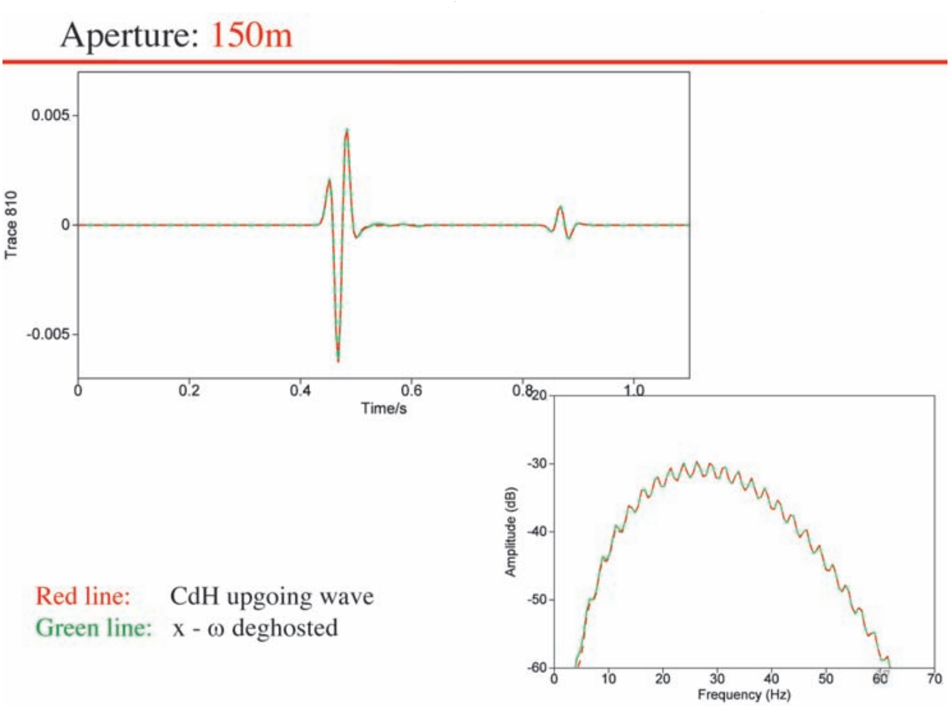
Aperture: 150m
0.005
0
-0.005
Trace 810
0
0.2
0.4
0.6
0.8
1.0
Time/s
Red line: CdH upgoing wave
Green line: x - ω deghosted
-20
-30
-40
-50
-60
Amplitude (dB)
0
10
20
30
40
50
60
70
Frequency (Hz)

Fig. 12.

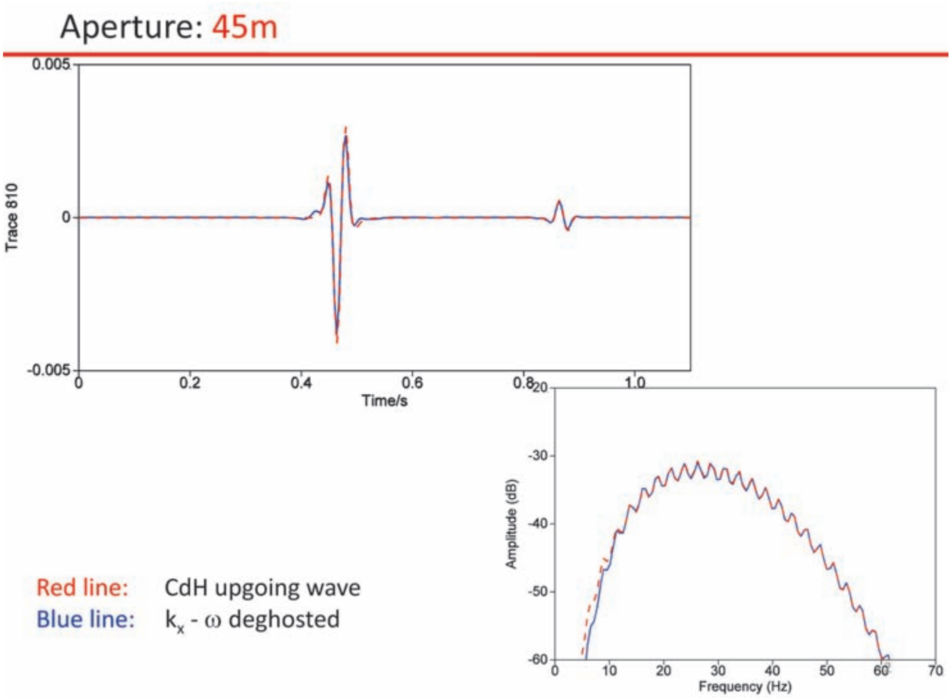
Aperture: 45m
0.005
0
-0.005
Trace 810
0
0.2
0.4
0.6
0.8
1.0
Time/s
Red line: CdH upgoing wave
Blue line: kx - ω deghosted
-20
-30
-40
-50
-60
Amplitude (dB)
0
10
20
30
40
50
60
70
Frequency (Hz)

Fig. 13.

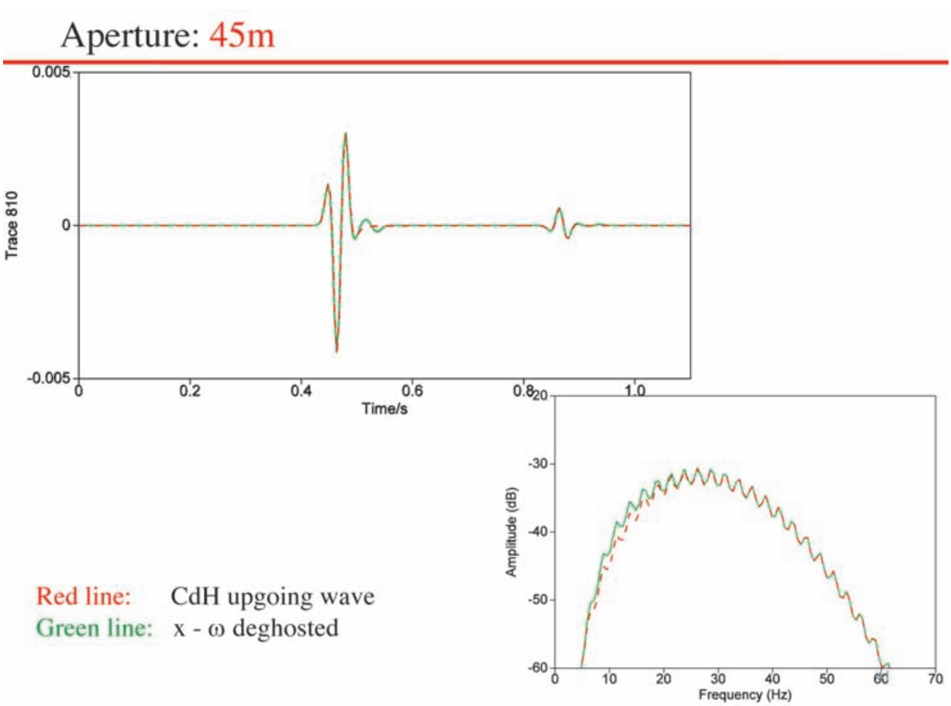
Aperture: 45m
0.005
0
-0.005
Trace 810
0
0.2
0.4
0.6
0.8
1.0
Time/s
Red line: CdH upgoing wave
Green line: x - ω deghosted
-20
-30
-40
-50
-60
Amplitude (dB)
0
10
20
30
40
50
60
70
Frequency (Hz)

Fig. 14.

ON-SHORE GREEN'S THEOREM WAVE FIELD SEPARATION: NEAR-SURFACE PROPERTIES

On-shore multiple attenuation can be an outstanding issue and significant challenge. Among issues that contribute to this pressing and high priority challenge are: (1) complex and ill-defined near-surface properties, (2) numerous and hard to identify multiple generators, and (3) interfering primaries and multiples. To address the latter issue, you need surgical removal of multiples so you don't damage the primaries, and that in turn requires capable delivery of the prerequisites required by inverse scattering series (ISS) multiple removal methods. To satisfy these prerequisites a set of Green's theorem procedures have been developed in, e.g., Weglein et al. (2002), Zhang and Weglein (2005, 2006), Zhang (2007), Mayhan et al. (2011, 2012), Mayhan and Weglein (2013), Tang et al. (2013), and others to separate the reference wave and scattered wave and to deghost. These procedures have shown value in synthetic data, SEAM data and marine field data (Zhang, 2007, Zhang and Weglein, 2005, 2006; Mayhan et al., 2012; Mayhan and Weglein, 2013). The biggest challenge is on land; how do we satisfy the prerequisites on land?

On land, the measurement surface is right on the perturbation, and the actual/energy source is on the same level/line as the measurements. We want to identify and remove the reference wave along with its surface waves. For on-shore application, the reference wave has surface waves, and Green's theorem can be a way to identify/use/remove surface waves. Today the petroleum industry often employs a combination of filter methods and intervention by capable processors. Surface wave identification/removal remains an open and important practical problem.

In the marine application of Green's theorem wavefield separation methods, we assume the air-gun source is above the cable and the output/prediction point is either above or below the measurement surface. For on-shore application the source can be on (or below) the measurement surface, and we might want the wave separation of the measured data itself. In Zhang (2007), Zhang and Weglein (2005), and Mayhan and Weglein (2013) it was shown that using the Green's theorem form [eq. (10)] that the output point must be more than $\frac{1}{2}\Delta x$ above the measurement surface, i.e., that $\Delta z = |z - z'_g| \geq \frac{1}{2}\Delta x$, where z is the output depth, z'_g is the cable depth, and Δx is the sampling interval. If it gets closer, the calculation becomes unstable, with empirically observed numerical issues. That numerical issue in the $(\mathbf{x},\omega)$ Green's theorem method precludes the output point being too close to the cable, and it cannot be on the cable itself. The requirement $\Delta z \geq \frac{1}{2}\Delta x$ holds for both Green's theorem $(\mathbf{x},\omega)$ deghosting and wavefield separation $(P = P_0 + P_s)$ for P_0 and P_s. However, since the $(\mathbf{k},\omega)$ Green's theorem deghosting methods, implicitly assume, in principle (in their derivations), perfect spatial sampling, $\Delta x = 0$, they provide algorithms/methods that allow the seismic source and/or the output/prediction point to be on the measurement surface.

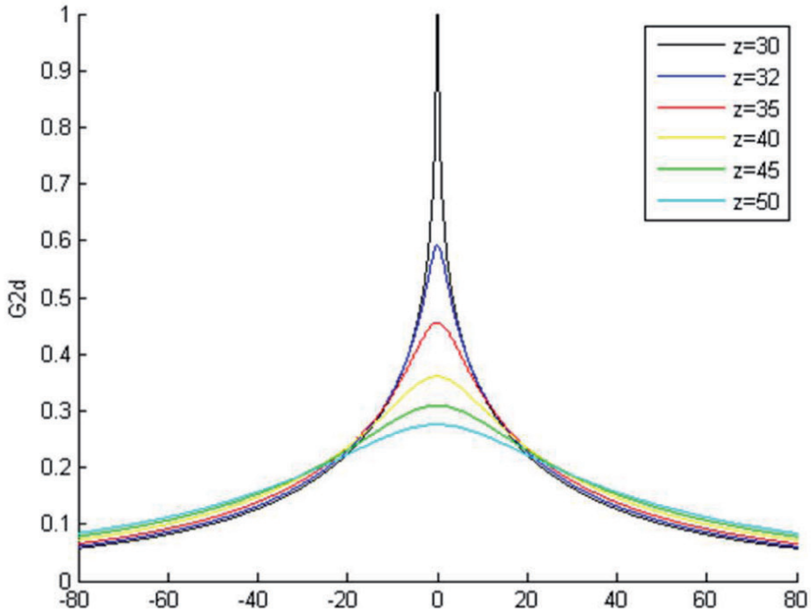

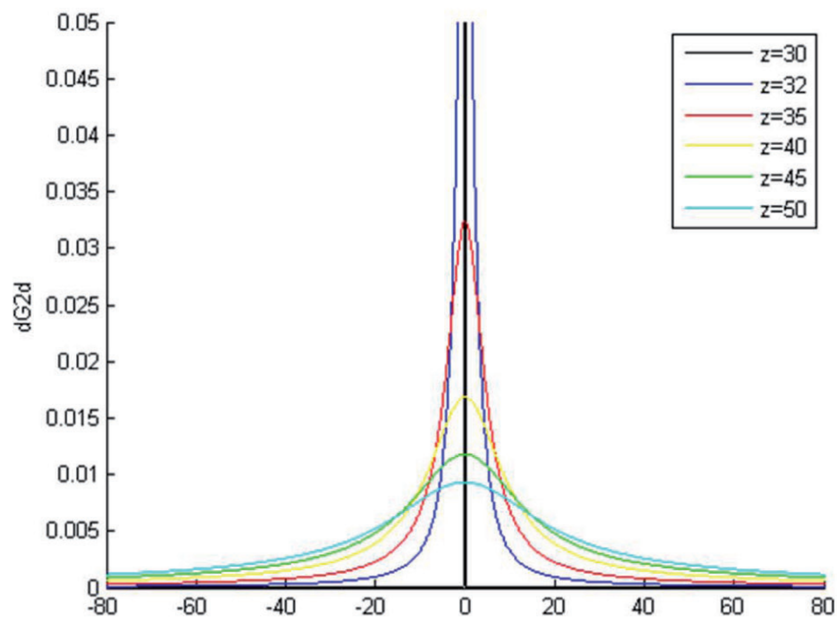

Fig. 15. The Green's function (top) and its normal derivative (bottom) as a function of the inline coordinate, x, and the depth, z, of the predicted wavefield below the air/water boundary.

Tang (2013) plotted the Green's function and its normal derivative as a function of the inline coordinate, x, and the depth, z, of the predicted wavefield below the air/water boundary. In Fig. 15, the left panel is $G_0(x,z,x'_g = 0, z'_g = 30, \omega = 25)$ and the right panel is $\partial G_0/\partial z(x,z,x'_g = 0, z'_g = 30, \omega = 25)$. x is the horizontal axis, and z is indicated by different colors. As z approaches z'_g, i.e., as the color changes from light blue to green to yellow to red to blue to black, $\partial G_0/\partial z$ becomes more narrow. Unless we have a small sampling interval Δx, the value of $\partial G_0/\partial z$ may not be picked up by the finite sum used to numerically approximate the integral, and the quality of deghosting falls off.

However, in the $P\text{-}V_z$, (or k_x,ω) domain, methods for wave field separation, when you Fourier transform, it assumes you have sampling sufficient to do the integral correctly without error. If you assume $\Delta x = 0$ as in $P\text{-}V_z$ forms, you can accommodate proximal to and on the cable for both the seismic source and output point.

The consequences of this difference between Green's theorem in $(\mathbf{x},\omega)$ and in $(\mathbf{k},\omega)$ or $(P\text{-}V_z)$ approaches are more significant than just wanting to deghost marine data on the cable. The difference between these two will assist us to deghost and wave separate on land. We will illustrate this using a simple example separating P_0 and P_s in a 1D earth with a normal incidence wave. In our example, we will further assume there is no earth, that P is P_0 and the scattered wave is zero. What if we want the source on the cable and the prediction point on the cable? Don't use eq. (10) directly; instead put eq. (10) (Weglein et al., 2002) in the Fourier domain. We will examine this issue in a 1D normal incidence example which is the same as being in the $(\mathbf{k},\omega)$ domain, since there is no x and no integral over x. Another question is how do we get P' on land? There are several ways we could imagine that requirement being satisfied. For example, if you are in the Middle East, one typically uses Vibroseis. The base plate has a phone and you can estimate something like a wavelet. From the wavelet and the field you get the derivative. $A(\omega)$, P, and P' are called the triangle; given two, the triangle will give you the third (Weglein and Amundsen, 2003, Corrigan et al., 1991).

FOR ON-SHORE APPLICATION: PLACING THE SOURCE AND THE OUTPUT POINT ON THE MEASUREMENT SURFACE

In Weglein and Secrest (1990) the Green's theorem reference wave, P_0, and scattered wave, P_s, separation analogous to eq. (10) becomes

$$\Big|_a^b\{P(dG_0^{d+}/dz') - (dG_0^{d+}/dz')\} = \begin{cases} -P_s & \text{above } z=a \\ P_0 & \text{below } z=a \end{cases} , \qquad (19)$$

where the reference medium is chosen (in this example) as a whole space of water $G_0^+ = G_0^{d+}$. The 1D normal incidence case in eq. (19) is the (k_x,ω) form when there is no x coordinate in the problem statement.

In the example, 'a' is chosen on the measurement surface on the surface of the earth, 'b' is below 'a', and z_s is above 'a'. The output point can be chosen to be above 'a' or below 'a'. Later in this example, we will make z_s on the surface of the earth, and our output point will be on 'a', as well. In the example, where the actual medium is a whole space of water, the output point above 'a' gives P_s and below 'a' gives P_0. And in this simple world, separating P_0 and P_s is also deghosting, because it is the same $G_0^+ = G_0^{d+}$. (For deghosting pick $G_0^+ = G_0^{d+}$. In general, deghosting and wavefield separation are not the same.) There is no P_s because there is no upgoing wave anywhere, including above z = a. The source wave is moving down so deghosting gives zero.

How to proceed when we want to apply Green's theorem wavefield separation methods where: (1) the source is on the measurement surface, and (2) we want to calculate P_s and P_0 in the data/on the cable. We know that we can not arrange that in the $(\mathbf{x},\omega)$ domain. Eq. (10) in $(\mathbf{x},\omega)$ forces you to stay above the cable (by an amount that depends on sampling), whereas in $(\mathbf{k},\omega)$ or P-V_z eq. (10) has in principle perfect sampling (Δx is zero) and hence the source and output points can be located on the measurement surface.

For transparency we consider the 1D normal incidence example. In eq. (19)

$$P = \exp(ik|z' - z_s|)/2ik \quad ,$$

$$dP/dz' = ik[\exp(ik|z' - z_s|)/2ik]\mathrm{sgn}(z' - z_s) \quad ,$$

$$G_0 = \exp(ik|z - z'|)/2ik \quad ,$$

$$dG_0/dz' = [ik\,\mathrm{sgn}(z' - z)/2ik]\exp(ik|z - z'|) \quad ,$$

$$\Big|_a^b\{[\exp(ik|z' - z_s|)/2ik]\{[\mathrm{sgn}(z' - z)/2]\exp(ik|z - z'|)\}$$

$$- [\exp(ik|z - z'|)/2ik]\exp(ik|z' - z_s|)\mathrm{sgn}(z' - z_s)/2\} \quad .$$

Evaluate at a < z < b. 'a' will contribute and 'b' won't contribute. This is shown below.

$$\{\exp[ik(b - z_s)]/2ik\}\overbrace{\{\mathrm{sgn}(b - z)}^{1}/2\}\exp[ik(b - z)]$$

$$- \{\exp[ik(b - z)]/2ik\}\exp[ik(b - z_s)]\overbrace{\mathrm{sgn}(b - z_s)}^{1}/2$$

$$- \{\{\exp[ik(a - z_s)]/2ik\}\overbrace{\{\mathrm{sgn}(a - z)}^{-1}/2\}\exp[ik(z - a)]$$

$$- \{\exp[ik(z - a)]/2ik\}\exp[ik(a - z_s)]\overbrace{\mathrm{sgn}(a - z_s)}^{1}/2\}$$

$$= \underbrace{\{\exp[ik(b-z_s)]/2ik\}\exp[ik(b-z)]/2 - \{\exp[ik(b-z)]/2ik\}\exp[ik(b-z_s)]/2}_{=0}$$

$$-\{\{\exp[ik(a-z_s)]/2ik\}\exp[ik(z-a)]/(-2) - \{\exp[ik(z-a)]/2ik\}\exp[ik(a-z_s)]/2\}$$

$$= (1/2ik)\exp[ik(z-z_s)] = P = P_0 \ . \qquad (20)$$

There is no contribution from b. The terms with b's cancel, and $P = P_0$ because the reference wave is the total wavefield. If we evaluate at $z_s < z < a$, the total contribution is zero because $P_0 = P$ and $P_s = 0$.

What do you do when you put the source on the cable? Fourier transforming into a k_x,ω form avoids the $\Delta z = ½\Delta x$ restriction because it begins with $P(k_x,z',x_s,z_s,\omega)$. No integral is left for x. The only question is where do you choose the output point, z? If you want to deghost on the cable, Fourier transform over x and use the P-V_z forms. The Dirac delta function properties are:

$$\int_V \delta(\mathbf{r} - \mathbf{r}')f(\mathbf{r}')d\mathbf{r}' = \begin{cases} f(\mathbf{r}) & \mathbf{r} \text{ in } V \\ 0 & \mathbf{r} \text{ outside of } V \end{cases} \ .$$

The application of Green's theorem methods to either the source or output point on the surface (the measurement surface) boils down to the question of what is $\int_V \delta(\mathbf{r} - \mathbf{r}')f(\mathbf{r}')d\mathbf{r}'$ when $\mathbf{r}$ is on the surface enclosing V. You can choose whether it's in or out of V (Morse and Feshbach, 1981, page 805). In our example above, evaluate at z_s = 'a', when the source is on the cable [$\mathrm{sgn}(z'-z_s) = \mathrm{sgn}(0)$], and if you want the source on the cable to be treated as the source above the cable, then choose $\mathrm{sgn}(a - z_s) = 1$ with $z_s = a$. For the output point, when $z = a$ (predict at the cable), if we want the same sign as when $z > a$, choose $\mathrm{sgn}(a - z) = -1$ when $z = a$. If you want the output point when it is on the surface (measurement surface) to be included with points above the cable choose $\mathrm{sgn}(a - z) = +1$ when $z = a$.

So our choice of sign will give P_0 or P_s on the cable, depending on whether you choose the cable to be included with the region below or above the cable, respectively. You're deciding whether the boundary is inside or outside the volume. You can't arrange this in eq. (10) because you can't get to the boundary, at least not while keeping the algorithm stable.

The bottom line here is for land you can't get close enough (to the boundary) to make a decision in eq. (10). This is not true if you go to the Fourier k_x,ω domain. But there is no free lunch. If Δx gets too big, $P(k_x,z,\omega)$ becomes inaccurate, and $P - V_z$ can have issues.

SUMMARY

Green's theorem $(\mathbf{x},\omega)$ deghosting methods for wave separation have advantages compared to Green's theorem deghosting in $(\mathbf{k},\omega)$ for non-horizontal measurement surfaces (ocean bottom, dipping cable). For applications where the interest is in wave separation on the cable itself and where the source is on the measurement surface (on-shore) $(\mathbf{k},\omega)$ would accommodate that interest whereas $(\mathbf{x},\omega)$ (Green's theorem) will not. This paper is examining the implication/differences of Green's theorem deghosting methods that operate in two domains: $(\mathbf{x},\omega)$ and $(\mathbf{k},\omega)$. Substituting the normal derivative of P in terms of the vertical component of velocity, V_z, in the $(\mathbf{k},\omega)$ domain, and benefits/limitations that arise from that substitution (while important) are not within the scope of this paper. There is work by Robertsson et al. (2008) and Amundsen et al. (2010) on the use of multicomponent streamer recordings for reconstruction of pressure wavefields in the crossline direction. Among open issues and challenges in Green's theorem wave separation preprocessing, for on-shore application, is the development of a new method and algorithm that can incorporate/combine the measurement surface shape flexibility of $(\mathbf{x},\omega)$ methods and the ability of $(\mathbf{k},\omega)$ methods to allow both the seismic source and the output point to be located on the receiver measurement surface.

ACKNOWLEDGEMENT

We thank the M-OSRP sponsors for their encouragement and support. We would like to thank Clark Trantham and Mamadou Diallo of ExxonMobil for stimulating discussions that motivated and encouraged this study.

REFERENCES

Amundsen, L., 1993. Wavenumber-based filtering of marine point-source data. Geophysics, 58: 1335-1348.

Amundsen, L., Weglein, A.B. and Reitan, A., 2013. On seismic deghosting using integral representation for the wave equation: Use of Green's functions with Neumann or Dirichlet boundary conditions. Geophysics, in press.

Amundsen, L., Westerdahl, H., Thompson, M., Haugen, J.A., Reitan, A., Landrø, M. and Ursin, B., 2010. Multicomponent ocean bottom and vertical cable seismic acquisition for wavefield reconstruction. Geophysics, 75: WB87-WB94.

Corrigan, D., A. B. Weglein, and D. D. Thompson. 1991 "Method and apparatus for seismic survey including using vertical gradient estimation to separate downgoing seismic wavefields.". US Patent number 5051961.

Mayhan, J.D., Terenghi, P., Weglein, A.B. and Chemingui, N., 2011. Green's theorem derived methods for preprocessing seismic data when the pressure P and its normal derivative are measured. Expanded Abstr., 81st Ann. Internat. SEG Mtg., San Antonio: 2722-2726. http://library.seg.org/doi/pdf/10.1190/1.3627759.

Mayhan, J.D. and Weglein, A.B., 2013. First application of Green's theorem-derived source and receiver deghosting on deep-water Gulf of Mexico synthetic (SEAM) and field data. Geophysics, 78: WA77-WA89. http://library.seg.org/doi/pdf/10.1190/geo2012-0295.1.

Mayhan, J.D., Weglein, A.B. and Terenghi, P., 2012. First application of Green's theorem derived source and receiver deghosting on deep water Gulf of Mexico synthetic (SEAM) and field data. Expanded Abstr., 82nd Ann. Internat. SEG Mtg., Las Vegas: 1-5. http://library.seg.org/doi/pdf/10.1190/segam2012-0855.1.

Morse, P.M. and Feshbach, H., 1981. Methods of Theoretical Physics. Original publication 1953 by The McGraw-Hill Companies, Inc. Feshbach Publishing, LLC, Minneapolis.

Robertsson, J.O.A., Moore, I., Vassallo, M., Özdemir, K., van Manen, D.J. and Özbek, A., 2008. On the use of multicomponent streamer recordings for reconstruction of pressure wavefields in the crossline direction. Geophysics, 73: A45-A49.

Tang, L., 2013. Green's theorem preprocessing and multiple attenuation: Acquisition configuration impact and determining the reference velocity for on shore application. Presentation given at 2012 M-OSRP Ann. Mtg., available online at mosrp.uh.edu.

Tang, L., Mayhan, J.D., Yang, J. and Weglein, A.B., 2013. Using Green's theorem to satisfy data requirements of multiple removal methods: The impact of acquisition design. Expanded Abstr., 83rd Ann. Internat. SEG Mtg., Houston.

Weglein, A.B. and Amundsen, L., 2003. Short note: G_0^{D0} and G_0^D integral equations relationships; The triangle relation is intact. M-OSRP 2002 Ann. Rep.: 32-35.

Weglein, A.B., Araújo, F.V., Carvalho, P.M., Stolt, R.H., Matson, K.H., Coates, R.T., Corrigan, D., Foster, D.J., Shaw, S.A. and Zhang, H., 2003. Inverse scattering series and seismic exploration. Inverse Probl., 19: R27-R83.

Weglein, A.B. and Secrest, B.G., 1990. Wavelet estimation for a multidimensional acoustic earth model. Geophysics, 55: 902-913.

Weglein, A.B., Shaw, S.A., Matson, K.H., Sheiman, J.L., Stolt, R.H., Tan, T.H., Osen, A., Correa, G.P., Innanen, K.A., Guo, Z. and Zhang, J., 2002. New approaches to deghosting towed-streamer and ocean-bottom pressure measurements. Expanded Abstr., 72nd Ann. Internat. SEG Mtg., Salt Lake City: 2114-2117.

Zhang, J., 2007. Wave theory based data preparation for inverse scattering multiple removal, depth imaging and parameter estimation: analysis and numerical tests of Green's theorem deghosting theory. Ph.D. thesis, Univ. of Houston.

Zhang, J. and Weglein, A.B., 2005. Extinction theorem deghosting method using towed streamer pressure data: analysis of the receiver array effect on deghosting and subsequent free surface multiple removal. Expanded Abstr., 75th Ann. Internat. SEG Mtg., Houston: 2095-2098.

Zhang, J. and Weglein, A.B., 2006. Application of extinction theorem deghosting method on ocean bottom data. Expanded Abstr., 76th Ann. Internat. SEG Mtg., New Orleans: 2674-2678.